Acta Medica
Okayama

Original Article

Image Quality of the Coronary Angiography with Noise Reduction Technology to Decrease the Radiation Dose

Masayuki Kumashiro[a,b], Takahiro Kataoka[a], Shinobu Yokota[b], Shinobu Nakagawa[b],
Keisuke Otsuki[b], Nobuyuki Miyake[b], Shinji Osumi[b], and Kiyonori Yamaoka[a]*

[a]*Graduate School of Health Sciences, Okayama University, Okayama 700-8558, Japan,*
[b]*Department of Radiological Technology, Kurashiki Central Hospital, Kurashiki, Okayama 710-8602, Japan*

We examined the effects of a reduced exposure dose on the quality of images from an angiography device augmented with a noise reduction algorithm. Before its clinical application, we compared the diameter of the discrimination limit of the hole with that in the conventional method by a visual evaluation with a contrast-detail (C-D) phantom imaged using the target dose. Based on the results, a reducible dose was determined and applied clinically. The sample population consisted of patients being followed up after percutaneous coronary intervention (PCI) for coronary artery disease; we evaluated the effects of the exposure reduction on image quality. A significant dose reduction was observed by the noise-reduction method compared to the conventional method; the radiation dose to the flat panel detector (FPD) could be reduced to 70 nGy per frame. Clinically, a dose reduction of approx. 40% was obtained while maintaining image quality almost equal to that of the conventional method.

Key words: image quality, radiation dose, noise reduction, percutaneous coronary intervention, contrast-detail phantom

Percutaneous coronary intervention (PCI) in patients with coronary artery disease has been an important development, but the increasing radiation exposure dose to both patients and operators is a problem [1-3]. Cases of skin disorders caused by an increase in the patient exposure dose due to prolonged fluoroscopy times and increased numbers of images were recently reported [4-8]. The International Commission on Radiological Protection (ICRP) and the U.S. Food and Drug Administration (FDA) have reported the effectiveness of the measurement and recording of exposure doses for patients for the prevention of the occurrence of skin disorders due to radiation [9-11].

According to the guidelines of the Radiation Safety in the Practice of Cardiology Writing Group Members, a PCI increases the risk of skin disorders. It is thus necessary to identify the safe radiation dose for PCIs, and staying below the threshold safe radiation dose is important [12].

In recent years, a system to reduce the radiation has been applied in clinical practice. The new technology uses an image noise reduction algorithm (Clarity IQ) specifically designed for X-ray images which combines a spatial filter and a temporal filter [13,14]. Both filters include an analysis operation that reveals the predominant structures in the image and excludes them from the filter phase. This approach is deployed at different spatial scales by using multiresolution image decomposition [15,16].

An angiography apparatus equipped with noise reduction technology (NRT) based on the Clarity IQ algorithm has been introduced and applied in clinical practice to reduce exposure during interventional radiology (IVR) procedures [17-21], resulting in dose reductions of >50%. However, these studies differ regarding the initial dose to be compared, the target dose reduction, the fluoroscopic time, and the frame number due to variations in physiques and in the procedure used, and thus comparisons of only the dose values versus reduction rates are inadequate.

The Clarity IQ noise reduction algorithm uses several functions to reduce the radiation dose. Noise reduction consists of both temporal and spatial noise reduction. Temporal noise reduction refers to processing performed over time and thus across subsequent images. Spatial noise reduction refers to processing performed over different regions within a single image. Temporal noise is reduced by averaging several frames. The Clarity IQ algorithm uses motion compensation by aligning moving structures before averaging. By utilizing this motion compensation, more frames can be used and more powerful temporal filtering can be applied. As a result, the noise of the moving structure is further reduced.

In the clinical application of these techniques, a significant reduction in the radiation dose causes a deterioration of the image quality due to X-ray quantum mottle; the signal buried in the noise component is more emphasized and the image quality deteriorates. It is necessary to determine how much the dose can be reduced without degrading the image quality.

The optimal ratio of image quality to radiation dose should be determined in accordance with the As Low As Reasonably Achievable (ALARA) principle. However, to the best of our knowledge there has been no report on how much the dose can be reduced in clinical applications, or on the verification of blood vessel visualization when clinically adopting the lowest dose acceptable for imaging diagnosis.

A previous study evaluated the image quality by switching consecutively from the conventional method to the Clarity IQ algorithm for the evaluation of the same patient [18], and the method had drawbacks of an increase in the radiation dose and contrast media for the patients. In the present study we conducted a similar comparison of the conventional method and the Clarity IQ algorithm within the context of a normal follow-up study that did not increase the patient burden. Our study also differs from other reports in terms of how much the radiation dose can be reduced from the target dose in a phantom experiment and in the clinical applications performed based on the phantom experiment.

Our aim was to determine how much noise reduction technology can reduce the radiation dose without degrading the image quality, by using a phantom examined with cine angiography equipment, and we applied the results clinically to verify the technology's usefulness.

Materials and Methods

Phantom study.

1. Contrast-detail phantom X-ray acquisition

For X-ray acquisition we used a commercially available 240 × 240 mm contrast-detail (C-D) phantom (Burger Phantom 41318-000, Kyoto Kagaku, Kyoto, Japan). This C-D phantom consists of concave hollow targets arranged in a matrix of 15 rows of 15 holes. The diameters and depths of these holes ranged from 1.0 mm to 8.0 mm (0.5-mm increments). Of these, the smallest identifiable hole diameter was defined as the identification limit diameter (ILD). Holes with diameters and depths of 1.0 mm to 4.5 mm were used to measure the ILD at each hole depth (Fig. 1).
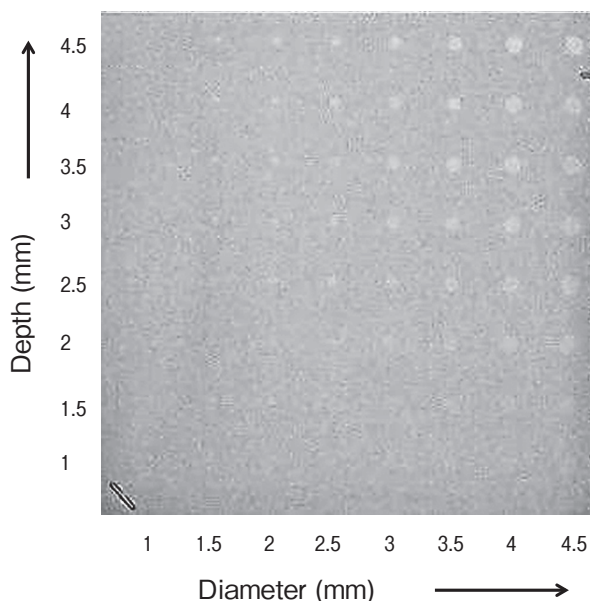

Fig. 1   Diameters and depths of the holes in the C-D phantom (concave type).

The first reference images were collected using a conventional flat panel detector (FPD) angiography apparatus (Allura FD 10; Philips Healthcare, Best, The Netherlands) with standard image processing and exposure system settings (the Xper 10; Philips Healthcare, Best, The Netherlands). Targeted study images were later collected using the same device with the noise reduction system (*i.e.*, the Clarity IQ algorithm; Philips Healthcare, Best, The Netherlands).

The experimental system consisted of a C-D phantom placed on 20-mm-thick acrylic resin and positioned so that the center of the phantom was an isocenter. The distance between the focus of the X-ray tube and the FPD was 105 cm. To obtain the same tube voltage and avoid differences due to X-ray energy, a large focus (0.8 mmφ) was used for the Xper system, and a small focus (0.5 mmφ) was used for the Clarity system. Copper (0.4-mm) and aluminum (1-mm) filters were added to the X-ray tube.

A total of 11 dose groups with an incident dose per frame on the FPD of 44-140 nGy/frame (nGy/f) in both systems were set based on the manufacturer's instructions. The irradiation conditions for obtaining these doses included a tube voltage of 70-76 kVp and a current of 496-821 mA, provided by the automatic exposure control (AEC) in the radiation imaging system. The actual incident dose (ID) per frame (frame rate: 15 frame/sec) was estimated from the dose area product (DAP) (mGy•cm^2) by the built-in area dosimeter. The DAP was obtained from the internal transmission ionization chambers (KermaX Plus; IBA Dosimetry, Schwarzenbruck, Germany) configured in each device.

2. Visual evaluation

We compared the quality of the images obtained by the Clarity method with the images obtained by the conventional Xper method and the ILD (in mm) of the cylinder of the C-D phantom. Five radiological technologists (M.K, K.O, S.N, N.M and S.Y) and 1 clinical engineering technician (T.S >10 years of experience among them) who routinely participate in quantitative coronary analyses (QCAs) in our hospital's angiography department acted as observers.

For the review, the acquisition image obtained by each method was displayed on a diagnostic quality image review monitor (MML1942-PER; Philips Healthcare). The images were presented to the reviewers in a random order, and the reviewers were blinded to the image characteristics. To maintain consistent observation conditions, the room lighting was constant, and the observations were performed under conditions automatically displayed on the image review monitor.

Differences in each ILD between the two acquisition methods were evaluated using a paired two-sided Student's *t*-test, and *p*-values < 0.05 were considered significant.

Clinical study.

1. Patients

This clinical study was conducted with the approval of the Ethics Committee of Kurashiki Central Hospital (no. 1563). The subjects were patients being followed up after a PCI. Immediately after the PCI the patients were examined with a conventional reference angiography device (Allura Xper FD 10 Biplane; Philips Healthcare); the follow-up examinations were performed within 2 years with a new device (Allura Clarity FD 10 Biplane; Philips Healthcare). Examinations with the conventional system were conducted between May 2011 and February 2013; examinations with the new system were conducted between January 2013 and March 2014.

Among these subjects, the 25 patients who did not experience a significant change (≥50%) in the stenosis rate in all 3 branches of the coronary artery were included in both studies. All 25 patients were examined within a routine protocol after giving informed consent. The demographics of the 25 patients were as follows: 21 males, 4 females; age: 70±10 years; BMI: 25.1±5.7 kg/m^2; period between examinations: 11.4±5.8 months. Among the final diagnoses, there were 9 cases of old myocardial infarction (OMI) and 16 cases of angina pectoris (AP); 24 patients underwent stent placement.

The examinations were performed by 16 cardiologists with >7 years of experience; the operator was not always the same before and after the examination of a patient. Contrast medium was injected using a 5-French diagnostic catheter; volumes of 7 mL in the left coronary artery (LCA) and 5 mL in the right coronary artery (RCA) were manually injected.

As a routine examination in all cases, radiographs were obtained from 8 directions for the LCA, 4 directions for the RCA, and 2 directions for the left ventricle (LV) with the biplane system. The imaging directions were as follows. For LCA: right anterior oblique (RAO), left anterior oblique (LAO) cranial, RAO caudal, LAO, anteroposterior (AP) cranial, LAO caudal,

RAO cranial, and AP caudal; for RCA: AP cranial, LAO, RAO caudal, and LAO cranial; and for LV: RAO and LAO.

The group that underwent cine angiography using the conventional angiography device was the "reference study (RS)" group; the group examined with the system equipped with the Clarity IQ algorithm was the "new study (NS)" group.

2. Clinical X-ray acquisition chain

In the reference study, the programmed exposure conditions were as follows: the imaging dose per frame was 120 nGy, the fluoroscopic dose was 40 nGy, and the tube voltage and current were determined by the automatic exposure unit on the largest field of view (8 inches). In the new study, the programmed exposure conditions were as follows: the imaging dose per frame was 70 nGy, the fluoroscopic dose was 34 nGy, and the tube voltage and current were given by the automatic exposure unit on the same field of view.

3. Visual evaluation

To determine the potential dose reduction, we compared each phantom image obtained by the device equipped with the noise reduction processing algorithm with the corresponding image obtained by the conventional method.

Images of the bilateral coronary arteries of 25 patients examined using both types of equipment were evaluated in randomized, blinded, offline readings. The images used for the visual evaluation were as follows: AP cranial 30° was used for the LCA and LAO 55° was used for the RCA. All images were displayed as pairs on the reference image monitor (MML 1942-PER, Philips). The observations were performed under conditions automatically displayed on the image review monitor; the images did not undergo post-processing. The observers were not notified of the characteristics of the image.

The images were evaluated in randomized, blinded, offline readings with cine images and still images obtained at the same angle. The anonymized images were displayed in pairs on 2 monitors (randomly on the left or right side). Seven experienced radiological technologists (M.K, K.O, D.S, S.N, N.M, S.O and S.Y > 10 years of experience in angiography) graded the coronary arteries (RCA and LCA) according to the criteria described herein. The evaluated image quality criteria were given a score of 1 to 5 as follows. 1, very poor: unsatisfactory for diagnosis; 2, mediocre: small

arteries not discernible at all and larger arteries not sharply defined; 3, average: fair vessel visualization that is useful for diagnosis, with distal parts of small arteries invisible; 4, good: good for visualization, with small vessels also visible; and 5, very good or excellent: superior visualization of the vasculature. Differences in each score between the 2 acquisition methods in the LCA and RCA were respectively evaluated using Wilcoxon rank sum test, and p-values < 0.05 were considered significant.

At the same time, the visibility of the peripheral small coronary arteries was also scored by 7 same technologists by comparing the NS and RS images. This score ranged from +2 to −2 as follows: +2, NS excellent; +1, NS good; 0, average; −1, RS good; −2, RS excellent. Similar evaluations were conducted by three cardiologists (S.K, M.O, and T.M) with > 10 years of experience in PCI, and we assessed the validity of the evaluation by the 7 technologists by performing a receiver operating characteristic (ROC) analysis and determining the area under the curve (AUC) based on the evaluation by the cardiologists. When at least 2 of the 3 cardiologists scored the peripheral small coronary arteries as +2, +1 or 0, we defined the signal as present (signal score 1). When a negative value was provided by 2 or more of the cardiologists, we defined the signal as absent (signal score 0). Differences in each score between the technologists and the cardiologists and also those between the LCA and RCA were evaluated using a paired two-sided Student's t-test; p-values < 0.05 were considered significant.

Statistical analyses were performed with EZR (Saitama Medical Center, Jichi Medical University), which is a graphical user interface for R (The R Foundation for Statistical Computing, ver. 1.33) [22].

4. Dose evaluation

For all 25 cases, the fluoroscopy times, total number of frames, DAP, and total air kerma (AK) in free air at each interventional reference point of the frontal and lateral devices were calculated on both types of equipment and compared. Each value was calculated using a paired two-sided Student's t-test; p-values < 0.05 were considered significant.

The conversion from DAP to AK (mGy) was made using a DAP calculation model [23]. The DAP is defined as the product of the area of the cross-section of the X-ray beam and the average AK over that cross-section. The implementation of the DAP calculation model can

be divided into 2 parts: the calibrated AK and the effective area of the beam. Specifically, the DAP is determined by a combination of the calibrated AK as a function of tube voltage and 4 pre-filters in the collimator, the heel effect of the X-ray tube, the shutter position, the wedges rotation and translation, the extra-focal radiation, and the collimator scatter contribution. In both the Xper and Clarity methods, the calibrated AK is measured as a function of the tube voltage with the different pre-filters.

As mentioned above, the DAP and AK can be determined by the built-in dosimeter, but we carried out our own dosimetric measurements (Accu-Gold; Radcal, Monrovia, CA, USA) in order to determine the actual AK rate (mGy/min) of both units in the fluoroscopy mode (fluoroscopic dose) and radiography mode (imaging dose). The installation point of the dosimeter was set at the IVR reference point based on International Electrotechnical Commission (IEC) standard 60601-2-43. In this case, the ID of the reference study was 130 nGy/f.

The correction coefficient (CC) between the measured and calculated values was determined, and the final dose reduction rates of DAP and AK were corrected based on this coefficient.

Results

Phantom study.   Table 1 shows the estimated incident dose per frame calculated with the built-in area dosimeter based on the Xper dose of 120 nGy/f. The error rate exceeded 5% at 70 nGy/f for Xper, 44 nGy/f and 60 nGy/f for Clarity.

Table 2 shows the average ILD for the depth of the C-D phantom at each dose of both systems. In the comparison of Xper and Clarity, the visibility in images taken using Clarity was excellent ($p < 0.04$) at all doses of 70 to 140 nGy/f at depths of 1 and 1.5 mm. A significant difference ($p < 0.03$) was observed at 70 nGy/f at a depth of 2 mm, but no significant difference was observed at 85 nGy/f, or at any dose at depths of ≥ 2.5 mm.

Table 3 shows the results of the comparison of ILDs between the Xper dose of 120 nGy/f and each Clarity dose. A significant difference was observed at 44 nGy/f at a depth of ≤ 2 mm and at 60 nGy/f at a depth of 1.5 mm or less ($p < 0.05$). However, in the comparison among the doses of 70, 79, and 85 nGy/f, there was no significant difference at any depth ($p > 0.17$). The lowest dose was estimated using the results of the visual evaluation; 70 nGy/f did not significantly affect the image quality.

The results of the comparison by the 6 observers of the ILD measurements at 70 and 120 nGy/f of both systems are illustrated in Fig. 2. Compared to Xper 120 nGy/f, the average ILD of Xper 70 nGy/f was significantly increased when the depth was ≤ 2mm ($p < 0.012$). However, in comparison with Clarity 70 nGy/f, the average ILD from 1 mm to 3.5 mm was equal or slightly increased; no significant difference was observed ($p > 0.17$). Based on these results, we used 70 nGy/f as a clinical dose reduction target.

Clinical study.
1. Visual evaluation
Table 4 summarizes the evaluation of the images of 25 patients by the seven observers. All images acquired

Table 1   The estimated incident dose (ID) per frame calculated with a built-in area dosimeter based on Xper 120 nGy/f

	ID (nGy/f)	Voltage (kV)	Current (mA)	DAP rate (mGy·cm²/f)	AK rate (mGy/f)	Normalized ID (nGy/f)	error (%)
Xper	70	74	518	8.67	0.122	74.7	6.8
	85	76	528	9.86	0.140	84.9	−0.2
	120	74	766	13.94	0.233	120.0	0.0
	140	75	814	15.74	0.229	135.5	−5.3
Clarity	44	70	496	6.31	0.090	54.4	23.7
	60	73	510	7.47	0.110	64.4	7.4
	70	74	518	8.37	0.120	72.1	3.0
	79	76	524	9.07	0.132	78.1	−1.2
	85	76	527	9.60	0.139	82.7	−2.8
	120	74	763	14.00	0.202	120.6	0.5
	140	75	821	15.90	0.230	136.9	−2.3

DAP, dose area product; AK, air kerma.

Table 2   The average values (standard deviations) of ILDs obtained by the six observers at 1.0–3.5 mm depth of the C-D phantom

ID (nGy/f)		ILDs (mm)					
	Depth (mm)	1	1.5	2	2.5	3	3.5
44	Clarity	3.08 (0.93)	2.17 (0.56)	1.67 (0.39)	1.33 (0.45)	1.17 (0.39)	1.00 (0.00)
60	Clarity	2.92 (0.76)	2.17 (0.56)	1.58 (0.56)	1.33 (0.45)	1.08 (0.39)	1.00 (0.00)
70	Xper	3.00 (0.57)	2.50 (0.45)	1.83 (0.48)	1.42 (0.50)	1.17 (0.39)	1.00 (0.00)
	Clarity	2.50 (0.61)	1.91 (0.67)	1.50 (0.45)	1.17 (0.39)	1.08 (0.39)	1.00 (0.00)
	P Value	<.01	<.05	<.05	NS	NS	NS
79	Clarity	2.42 (0.69)	1.83 (0.56)	1.50 (0.45)	1.17 (0.39)	NS	1.00 (0.00)
85	Xper	3.08 (0.53)	2.42 (0.38)	1.58 (0.56)	1.25 (0.48)	1.08 (0.39)	1.00 (0.00)
	Clarity	2.25 (0.64)	1.67 (0.70)	1.42 (0.50)	1.17 (0.39)	1.00 (0.00)	1.00 (0.00)
	P Value	<.01	<.05	NS	NS	NS	NS
120	Xper	2.50 (0.45)	1.83 (0.38)	1.33 (0.45)	1.08 (0.39)	1.00 (0.00)	1.00 (0.00)
	Clarity	2.17 (0.56)	1.50 (0.61)	1.25 (0.48)	1.08 (0.39)	1.00 (0.00)	1.00 (0.00)
	P Value	<.05	<.05	NS	NS	NS	NS
140	Xper	2.42 (0.38)	1.75 (0.49)	1.33 (0.45)	1.08 (0.39)	1.00 (0.00)	1.00 (0.00)
	Clarity	2.08 (0.45)	1.41 (0.50)	1.08 (0.39)	1.00 (0.00)	1.00 (0.00)	1.00 (0.00)
	P Value	<.05	<.05	NS	NS	NS	NS

Values are given as mean (standard deviation) or number. ILD, identification limit diameter.

Table 3   Comparison of IDLs between Xper 120 nGy/f and each ID of clarity

ID (nGy/f)		ILDs (mm)			
	Depth (mm)	1	1.5	2	2.5
Xper	120	2.50 (0.45)	1.83 (0.38)	1.33 (0.45)	1.08 (0.39)
Clarity	44	3.08 (0.93)*	2.17 (0.56)*	1.67 (0.39)*	1.33 (0.45)
Clarity	60	2.92 (0.76)*	2.17 (0.56)*	1.58 (0.56)	1.33 (0.45)
Clarity	70	2.50 (0.61)	1.91 (0.67)	1.50 (0.45)	1.17 (0.39)
Clarity	79	2.42 (0.69)	1.83 (0.56)	1.50 (0.45)	1.17 (0.39)
Clarity	85	2.25 (0.65)	1.67 (0.76)	1.42 (0.50)	1.17 (0.39)
Clarity	120	2.17 (0.56)*	1.50 (0.61)*	1.25 (0.48)	1.08 (0.39)

Values are given as mean (standard deviation) or number. *p <.05. ID, incident dose.
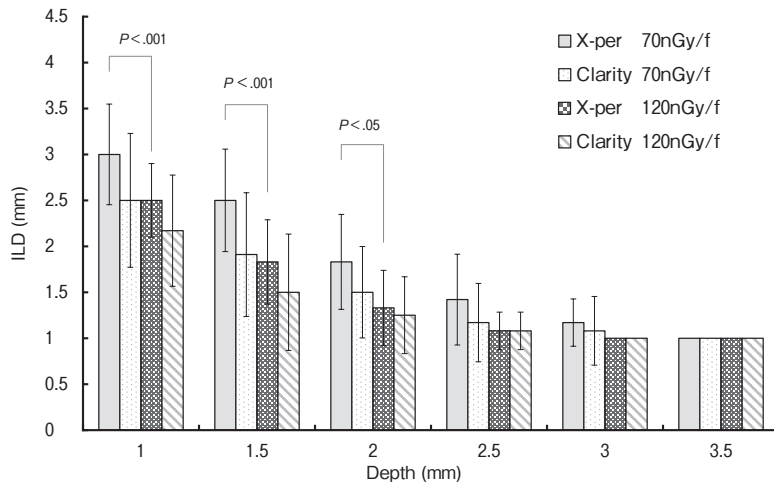
Fig. 2   The average identification limit diameter (ILD) at each hole depth in the C-D phantom.

in this study were of diagnostic quality and were used to assess clinically relevant information.

In the LCA evaluation, none of the 7 observers observed any significant difference between the RS and NS. The average of the NS (*i.e.*, 3.70) was almost the same as the average value of the RS (3.71). In the RCA evaluation, one observer reported a significant decrease in the NS, but the others did not recognize a significant difference between the RS and NS. Although the average value of the RS was 3.58, the average of NS was reduced to 3.33, but the difference was not significant ($p = 0.062$). Typical LCA cases are shown in Fig. 3, and typical RCA cases are shown in Fig. 4.

Panels A and B of Fig. 5 compare the evaluation of images by the 7 technologists between the LCA and RCA for the 25 patients. In the LCA, 62% of the new study (NS) images were evaluated as excellent, good, or equivalent (non-inferior) compared to the reference study (RS) images (excellent: 7%; good: 29%; average: 26%). In the RCA, 47% of the NS images were evaluated as excellent, good, or equivalent (non-inferior) compared to the RS images (excellent: 6%; good: 23%; average: 18%).

Table 5 compares the evaluation scores of the LCA and RCA given by the technologists and cardiologists. The LCA score was −0.02 for the technologists and 0.12 for the cardiologists, and the RCA score was −0.29 for the technologists and −0.15 for the cardiologists; the cardiologists' scores were somewhat higher for both the LCA and RCA, but significant differences were not observed between the 2 groups (LCA: $p = 0.255$; and RCA: $p = 0.250$). The AUCs were 0.840 (95%CI 0.616-1.000) in the LCA and 0.849 (95%CI 0.696-1.000) in the RCA, which suggested that the results of the evaluation by the technologists were almost the same as those of the evaluation by the cardiologists with high probability. For the LCA, the sensitivity was 0.900 and the specificity was 0.800, with a threshold value of 2.571 (Fig. 6A). For the RCA, the sensitivity was 0.769 and the specificity was 0.917, with a threshold value of 3.000 (Fig. 6B).

2. Dose evaluation

Table 6 shows the calculated and measured AK rates (mGy/min) of both systems for each fluoroscopic and imaging dose. Both the measured and calculated values

**Table 4** Diagnostic image quality obtained by the 7 technologists

	Observer	Score							
		A	B	C	D	E	F	G	Average
LCA	Reference	3.88 (0.65)	3.80 (0.74)	3.44 (0.80)	3.60 (0.71)	3.88 (1.11)	3.60 (0.71)	3.80 (0.74)	3.71 (0.62)
	New	3.64 (0.76)	3.44 (0.69)	3.68 (0.76)	3.84 (0.67)	4.00 (1.14)	3.44 (0.69)	3.88 (0.65)	3.70 (0.61)
	P Value	NS	NS	NS	NS	NS	NS	NS	NS
RCA	Reference	3.64 (0.81)	3.28 (0.80)	3.52 (0.86)	3.40 (0.79)	4.04 (1.16)	3.44 (0.85)	3.72 (0.75)	3.58 (0.71)
	New	3.40 (0.88)	3.00 (0.69)	3.24 (0.78)	3.20 (0.91)	3.48 (1.24)	3.20 (0.77)	3.24 (0.78)	3.33 (0.71)
	P Value	NS	NS	NS	NS	NS	NS	<0.01	NS

Values are given as mean (standard deviation) or number.
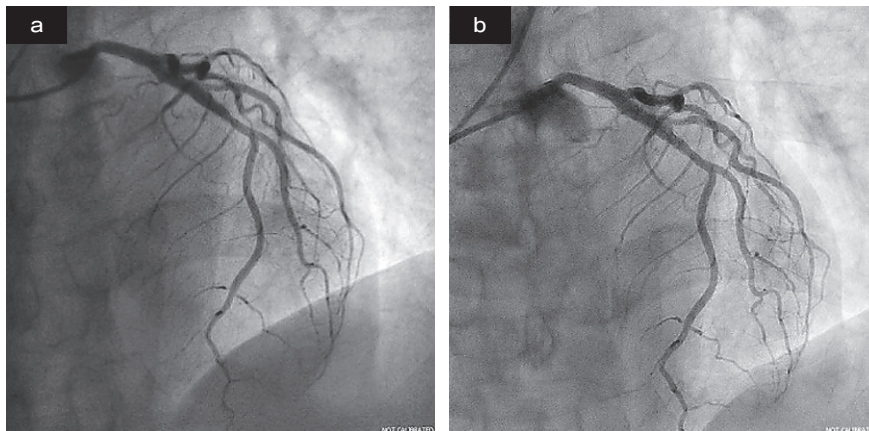
Fig. 3A The LCAs of the patient with AP: a 66-year-old male, BMI = 25.1, plain old balloon angioplasty [POBA], left anterior descending artery [LAD]#7). Average grading score (**a** = 3.57 < **b** = 3.85). **a** = reference study (RS), **b** = new study (NS).
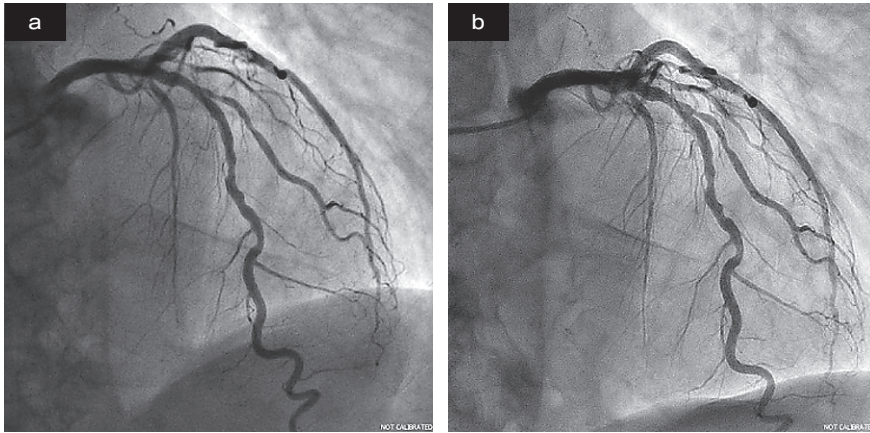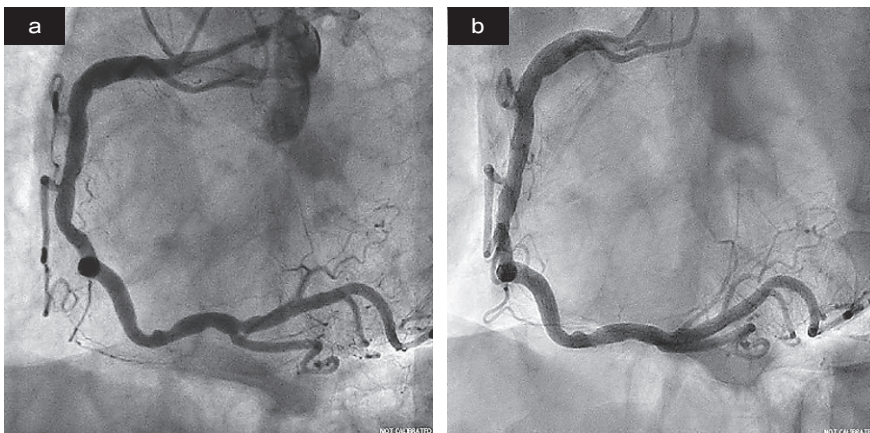
Fig. 3B The LCAs of the patient with AP: a 79-year-old male, BMI = 22.4, stent LAD#6 and left circumflex (LCX)#13, POBA LAD#9. Average grading score: a [RS] = 4.00 > b [NS] = 3.85.
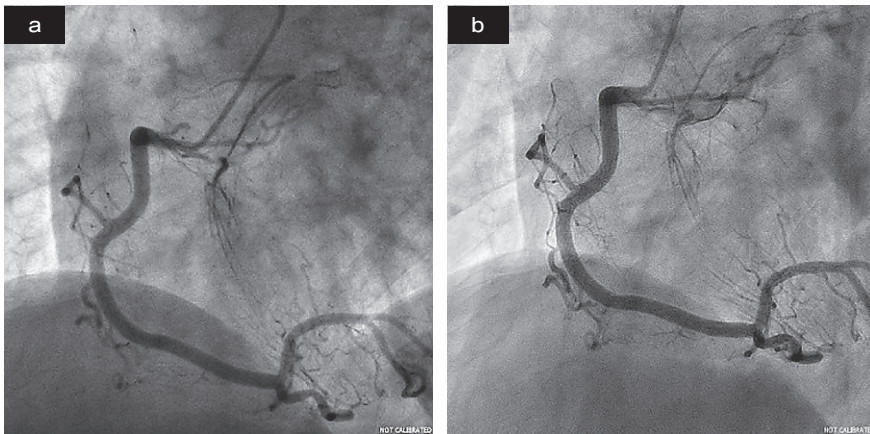
Fig. 4A The RCAs of the patient with AP: a 66-year-old male, BMI = 25.1. Average grading score (a [RS] = 3.14 < b [NS] = 4.00).

Fig. 4B The RCAs of the patient with AP: a 79-year-old male, BMI = 22.4, POBA RCA#2. Average grading score, a [RS] = 4.00 > b [NS] = 3.14.

in the fluoroscopic dose reference system were consistent at 27 mGy/min. However, in the new system, the measured value increased to 23 mGy/min compared to the calculated value of 21 mGy/min (CC 1.095). In addition, in the reference system of the imaging dose, the calculated value was approx. 174 mGy/min and the measured value of 173 mGy/min was approximately the same (CC 0.995). However, in the new system, the measured value decreased to 91 mGy/min compared to the calculated value of 95 mGy/min (CC 0.958). It was thus necessary to correct the DAP value by a 9.5% increase in the fluoroscopic dose but by a 4.2% decrease
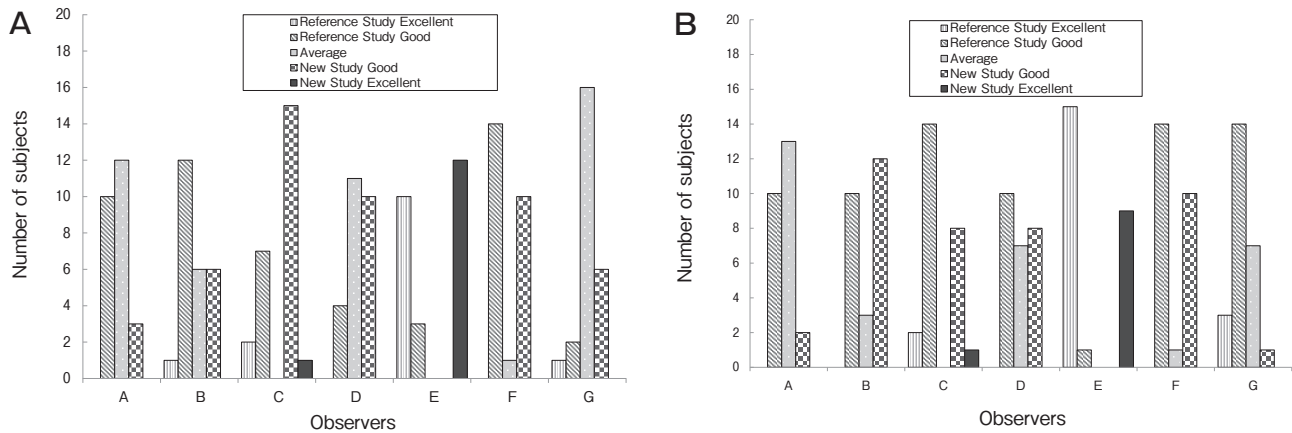
Fig. 5   The relative evaluation of images of the LCAs (left) and RCAs (right) of 25 patients by the 7 observers, comparing the reference and new studies.

Table 5   Relative image quality obtained by the 7 technologists and 3 cardiologists

	Technologists	Cardiologists	P Value	AUC	95%CI
LCA	−0.02 (0.72)	0.12 (0.65)	NS	0.840	0.616−1.000
RCA	−0.29 (0.73)	−0.15 (0.49)	NS	0.849	0.696−1.000
P Value	NS	< 0.01			

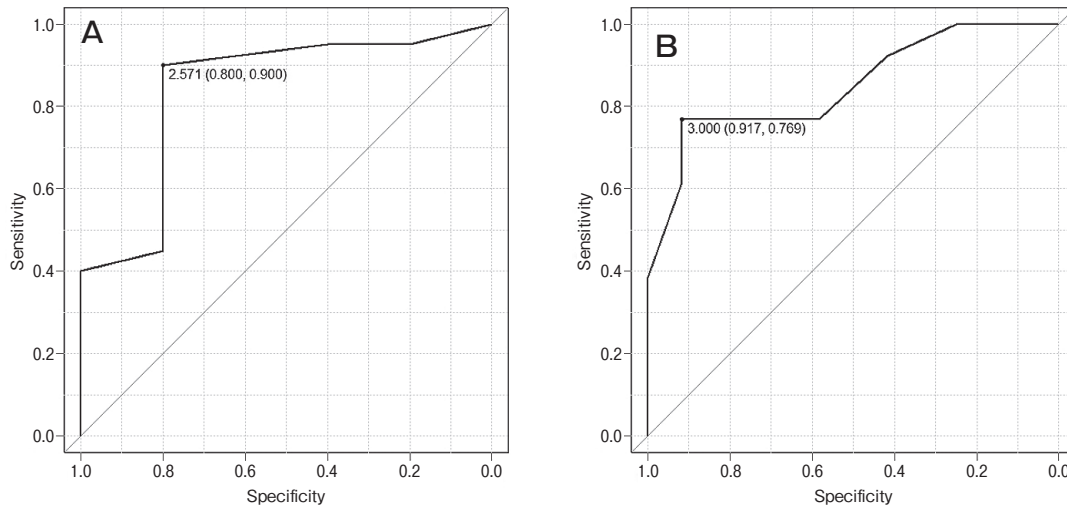Values are given as mean (standard deviation) or number. AUC, area under the curve.

Fig. 6   ROC curves in the LCA, (left) and the RCA (right).

in the imaging dose.

Table 7 shows the average values and standard deviations (SDs) of the fluoroscopic time (min), the number of imaging frames, the DAP rate (mGy•cm²/f), and the front and lateral AK (mGy). The average fluoro-

scopic time was 6.1 min in the reference study and 6.2 min in the new study; the difference was not significant ($p = 0.426$). The average number of frames in the new study was 1,717, which was slightly higher than the 1,661 of the reference study, but the difference was

Table 6　The calculated and measured dose rates in the Xper and Clarity systems for each fluoroscopic and imaging dose

		Calculated AK rate (mGy/min)	Measured AK rate (mGy/min)	Correction Coefficient	Error (%)
Fluoroscopic Dose	Xper	27	27	1.000	0.0
	Clarity	21	23	1.095	9.5
Imaging Dose	Xper	174	173	0.995	−0.5
	Clarity	95	91	0.958	−4.2

Table 7　The average values and SDs of fluoroscopic time (min), number of imaging frames, DAP per frame (mGy·cm^2/f), and front and lateral AKs (mGy)

		Reference Study	New Study	P Value
Fluoroscopic Time (min)		6.1 (3.6)	6.2 (4.2)	NS
Frame Number		1661 (294)	1717 (227)	NS
DAP rate (mGy·cm^2/f)	Complete Study (n = 25)	24.1 (6.9)	14.8 (4.2)	< .001
	BMI < 25 kg/m^2 (n = 13)	20.6 (5.8)	12.5 (3.5)	< .001
	BMI > 25 kg/m^2 (n = 12)	27.9 (8.6)	17.4 (5.0)	< .001
AK-F (mGy)		306 (106)	216 (87)	< .001
AK-L (mGy)		493 (174)	326 (140)	< .001

Values are given as mean (standard deviation) or number. DAP, dose area product; AK-F, air kerma in frontal system; AK-L, air kerma in lateral system.

not significant ($p = 0.140$).

In the new complete study, the average DAP rate was significantly reduced by 39% (24.1 to 14.8 mGy·cm^2/f, $p < 0.001$), and the reduction rate estimated by the correction coefficient obtained from the measured value was 40% (23.9 to 14.2 mGycm^2/f), which agreed with the 40% reduction rate (120 to 72.1 nGy/f) of the ID corrected with the phantom experiment. Similarly, the average value of the AK decreased by 29% (306 to 216 mGy) in the frontal system and by 34% (493 to 326 mGy) in the lateral system. A total decrease of 32% was confirmed, and the difference was significant ($p < 0.001$).

Discussion

The results obtained from the phantom experiments suggested that the new cine angiography system using noise reduction technology (NRT) can be used to reduce the dose without degrading image quality, even if the dose is reduced by about 40%. Next, therefore, we applied the new system in a clinical setting, and our findings demonstrated that it is possible to reduce the imaging dose to 40% while maintaining a nearly equal image quality. We observed that the incident dose to the FPD could be reduced from 120 to 70 nGy per frame. Deterioration of the image was observed at ≤60 nGy,

and we estimated that there was a clear branch point caused by degradation of the image quality due to X-ray quantum mottle between 60 and 70 nGy.

Because there was no temporal fluctuation in the phantom experiment using the Clarity IQ device, attention should be focused only on the influence of spatial noise. Since the spatial noise filter detects noise in a single image and filters on a pixel-by-pixel basis, neighboring pixels should be considered. It is therefore possible to enhance only the signal strength. We thus speculate that the Clarity IQ algorithm can obtain the same images as Xper but at a lower dose. However, below a certain dose, the influence of quantum mottle increases and the signal becomes buried in noise components. In this situation, we cannot separate the pixel intensity of the signal and the noise; it seems that the signal is averaged together with the noise and the rendering ability is reduced.

To reduce the exposure dose of the patients and operators, it is necessary to optimize the dose and perform image quality evaluations using phantom experiments. Using the C-D phantom, we determined the minimum dose required for cine angiography that is necessary to maintain the quality of the image by the ILD. This constitutes another unique application of the exposure reduction technology to clinical practice. However, the disadvantage of this technique is that it

only evaluates the ILD, not the discriminable minimum contrast (discrimination contrast) in the contrast-detail diagram (C-D curve) method [24]. It was impossible to evaluate the small size when the depth was ≥2.5 mm, as the disk was up to 1 mm in diameter.

Although this method can easily perform relative comparisons, such as the influence of various parameters on images, it depends on subjective judgment criteria, so it is likely to be affected by observation conditions. In the visual evaluation of the C-D phantom, the standard deviation of the ILD was a maximum of 0.93 in the low-dose range and the error was large. This may also be attributed to the fact that the window and level could not be freely selected so that the observer could easily evaluate the signal to maintain constant observation conditions. It seems necessary to compare the objective visual evaluation methods such as ROC [25] and the physical evaluation.

In dose assessments, an AK value is displayed as the sum of the imaging and fluoroscopic doses, whereas the DAP shows the individual photograph and the fluoroscopic doses. In our study, the fluoroscopic dose was reduced by 15%, from 40 nGy/f to 34 nGy/f, to maintain the visibility of the guidewire during a PCI. The reduction rate of the AK was thus lower than that of the DAP by an average of 32% on the front and side faces.

Cate *et al.* [18] evaluated the area dose per frame; in 39 cases (average BMI = 26.4 kg/m^2) the patient's DAP was reduced from 55 to 26 mGy•cm^2/f. According to our present data, the DAP of 25 patients (average BMI = 25.1 kg/m^2) was reduced from 24 to 15 mGy•cm^2/f. In our study, the dose was further reduced by approx. 42%, which was due to differences in the physiques of Western and Japanese patients. It is also necessary to consider that the reduction value used in this study was a limited dose range. In fact, Cate *et al.* [18] reported that overall, 85% of the image sets were considered to be of better or equal (non-inferior) quality compared to the reference cine. However, in our study the percentages of image sets better or equal to the reference cine were 62% for LCA and 47% for RCA, or less than half the sets in the latter case.

The relative score was −0.02 in the LCA and −0.29 in the RCA, and the evaluation was slightly inferior in the RCA. In our clinical assessment, we used the ROC method to investigate the authenticity of the technologists' evaluation. However, our ROC evaluation verified the reliability of the technologists' evaluation by

comparing the judgment criteria of the cardiologists as the true signal and the signal in normal angiography, and it did not directly compare the visibility between Xper and Clarity. The more images which were highly evaluated by the reviewer in both comparisons, we consider that the visualization capability is excellent system with a high probability. The finding that 62% (LCA) and 47% (RCA) of the image sets were evaluated as equivalent or better in our study did not exceed the results by the conventional method. We thus consider the 2 systems nearly equivalent.

The lower value of the RCA compared to the LCA was shown by the Xper of the conventional method as well as by the Clarity. The fundamental differences that are common to both systems may be due to differences in the amount of contrast agent, differences in the imaging angle, and the influence of the AEC. We used a large focus on Xper and a small focus on Clarity, and thus using a small focus on the X-ray tube, the voltage was increased due to the action of the AEC in the patients with a high BMI. We speculate that along with the rise in the tube voltage, the deterioration of image quality is due to a reduction of contrast and an increase of scattered X-rays.

In the visual evaluation of the RCA by the 7 technologists, the score was ≤3 in 4 of the 25 cases; the average BMI of these 4 patients was 29.7 kg/m^2, which is higher than the average value of the 25 cases (25.1 kg/m^2). We suspect that the tube voltage was changing to the high-voltage side in these 4 cases. As the target dose was set to the lowest dose range, in the case of halation within the field of view or an insufficient degree of inspiration by the patient or an overlap of the vertebral bodies and other organs, we speculated that the required dose could not be obtained due to the automatic exposure function. In these cases, it seems necessary to consider the dose-range setting assumptions.

Although our study used the same cases, the examination was performed by 16 cardiologists who differed between the 2 parts of the studies. Since influences due to differences in fluoroscopic time among operators have also been reported [20], it is also necessary to consider the influence of operator differences. In addition, since there was an interval of approx. 11 months (max. 23 months) between examinations, the patients' information also changed, and thus a complete comparison is difficult.

To exclude these factors, Cate *et al.* [18] performed

contrast examinations at the same angle twice consecutively in the same patient. Although the reproducibility of both examinations was maintained, there is concern about an increase in the exposure dose and contrast medium. A sufficient explanation for the patient and his/her agreement are necessary, and it is difficult to implement this without patient cooperation.

Our facility uses a biplane system; there are reports that biplane systems are expected to reduce the contrast agent and other reports that the exposure dose will increase [26, 27]. However, targeted blood vessels and stenosis sites have been identified in followed-up patients and others who are repeatedly examined. As patient information also continues to be updated, it is more likely that the benefit of radiation reduction will compensate for the slight decrease in image quality.

In conclusion, we used a phantom to investigate whether a decrease in the radiation dose could be achieved by using noise reduction technology in the angiography apparatus. Our results demonstrated that it is possible to reduce the incident dose to the FPD dose to 70 nGy per frame. We applied the technique to patients after a follow-up PCI, and a dose reduction of approx. 40% was achieved while image quality was essentially maintained.

References

1. ICRP Publication 59: The biological basis for dose limitation in the skin, Ann ICRP 22(2): (1992).
2. Shope TB: Radiation-induced skin injuries from fluoroscopy. Radiographics (1996) 16: 1195–1199.
3. ICRP Publication 85: Avoidance of radiation injuries from medical interventional procedures, Ann ICRP 30(2): (2000).
4. Wagner LK, Eifel PJ and Geise RA: Potential biological effects following high X-ray dose interventional procedures. J Vasc Interv Radiol (1994) 5: 71–84.
5. Koenig TR, Wolff D, Mettler FA and Wagner LK: Skin injuries from fluoroscopically guided procedures: part 1, characteristics of radiation injury. AJR Am J Roentgenol (2001)177: 3–11.
6. Koenig TR, Mettler FA and Wagner LK: Skin injuries from fluoroscopically guided procedures: part 2, review of 73 cases and recommendations for minimizing dose delivered to patient. AJR Am J Roentgenol (2001) 77: 13–20.
7. Berlin L: Radiation-induced skin injuries and fluoroscopy. AJR Am J Roentgenol (2001) 177: 21–25.
8. Suzuki S, Furui S, Kohtake H, Yokkoyama N, Kozuma K, Yamamoto Y and Isshiki N: Radiation exposure to patient's skin during percutaneous coronary intervention for various lesions, including chronic total occlu-
sion. Circ J (2006) 70: 44–48.
9. ICRP Publication 103: The 2007 Recommendations of the International Commission on Radiological Protection. Ann ICRP (2007).
10. ICRP Publication 113: Education and Training in Radiological Protection for Diagnostic and Interventional Procedures. Ann ICRP (2009).
11. FDA Public health Advisory: Avoidance of serious X-ray-induced skin injuries to patients during fluoroscopically-guided procedures; U.S. Food and Drug Administration (FDA), September 9 (1994), online publication: 1–7.
12. Guideline for Radiation Safety in Interventional Cardiology. (JCS 2011) Digest Version: JCS Joint Working Group, Advance Publication by-J-STAGE, Released online January 10 (2013): 1–31.
13. Söderman M, Holmin S, Andersson T, Palmgren C, Babic D and Hoomaert B: Image noise reduction algorithm for digital subtraction angiography: clinical results. Radiology (2013) 269: 553–560.
14. Dekker LR, van der Voort PH, Simmers TA, Verbeek XA, Bullens RW, Veer MV, Brands PJ and Meijer A: New image processing and noise reduction technology allows reduction of radiation exposure in complex electrophysiologic interventions while maintaining optimal image quality: a randomized clinical trial. Heart Rhythm (2013) 10: 1678–1682.
15. Jago J, Collet-Billon A, Chenal C, Jong JM and Makram-Ebeid S: XRESs: adaptive enhancement of ultrasound images. Medicamundi (2002) 46: 36–41.
16. Meuwly JY, Thiran JP and Gudinchet F: Application of adaptive image processing technique to real-time spatial compound ultrasound imaging improves image quality. Invest Radiol (2003) 38: 257–262.
17. Bracken JA, Mauti M, Kim MS, Messenger JC and Carroll JD: A radiation dose reduction technology to improve patient safety during cardiac catheterization interventions. J Interv Cardiol (2015) 28: 493–497.
18. ten Cate T, van Wely M, Gehlmann H, Mauti M, Camaro C, Reifert N, Suryapranata H and de Boer MJ: Novel X-ray image noise reduction technology reduces patient radiation dose while maintaining image quality in coronary angiography. Neth Heart J (2015) 23: 525–530.
19. Eloot L, Thierens H, Taeymans Y, Drieghe B, De Pooter J, Van Peteghem S, Buytaert D, Gijs T, Lapere R and Bacher K: Novel X-Ray Imaging technology enables significant patient dose reduction in interventional cardiology while maintaining diagnostic image quality. Catheter Cardiovasc Interv (2015) 86: E205–E212.
20. Nakamura S, Kobayashi T, Funatsu A, Okada T, Mauti M, Waizumi Y and Yamada S: Patient radiation dose reduction using an X-ray imaging noise reduction technology for cardiac angiography and intervention. Heart Vessels (2016) 31: 655–663.
21. Kastrati M, Langenbrink L, Piatkowski M, Piatkowski M, Michaelsen J, Reimann D and Hoffmann R: Reducing Radiation Dose in Coronary Angiography and Angioplasty Using Image Noise Reduction Technology. Am J Cardiol (2016) 118: 353–356.
22. Kanda Y: Investigation of the freely available easy-to-use software 'EZR' for medical statistics. Bone Marrow Transplantation (2013) 48: 452–458.
23. Maria M and Jan J: Dap calculation model An evolution in Dose Product indication. Interventional X-ray; Philips Healthcare, The Netherlands, Printed in The Netherlands 45220962099541, Dec (2013): 1–7.
24. Loo LN, Doi K, Ishida M, Metz CE, Chan HP, Higashida Y and Kodera Y: An empirical investigation of variability in contrast-detail diagram measurements. Proc SPIE (1983) 419: 68–76.
25. Goodenough DJ, Rossmann K and Lusted LB: Radiographic application of receiver operating characteristics (ROC) cures. Radiology (1974) 110: 85–95.
26. Lin A, Brennman P, Sadick N, Kovoor P, Lewis S and Robinson JW: Optimisation of coronary angiography exposures requires a multifactorial approach and careful procedural definition. Br J Radiol (2013) 86: 20120028.
27. Sadick V, Reed W, Collins L, Sadick N, Heard R and Robinson J: Impact of biplane versus single-plane imaging on radiation dose, contrast load and procedural time in coronary angioplasty. Br J Radiol (2010) 83: 379–393.